*Articles*

# Catalytic and Chemical Competence of Regulation of Cdc25 Phosphatase by Oxidation/Reduction†

Jungsan Sohn and Johannes Rudolph*

*Departments of Biochemistry and Chemistry, Duke University Medical Center, Durham, North Carolina 27710*

*Received March 31, 2003; Revised Manuscript Received June 9, 2003*

ABSTRACT: Cdc25 phosphatases belong to the family of protein tyrosine phosphatases (PTPs) that contain an active-site cysteine and form a phosphocysteine intermediate. Recently, oxidation/reduction of active-site cysteines of PTPs, including Cdc25, has been proposed to serve as a form of reversible regulation for this class of enzymes. Here we provide in vitro evidence that supports the chemical and kinetic competence for oxidation/reduction of the active-site cysteines of Cdc25B and Cdc25C as a mechanism of regulation. Using kinetic measurements and mass spectrometry, we have found that the active-site cysteines of the Cdc25's are highly susceptible to oxidation. The rate of thiolate conversion to the sulfenic acid by hydrogen peroxide for Cdc25B is 15-fold and 400-fold faster than that for the protein tyrosine phosphatase PTP1B and the cellular reductant glutathione, respectively. If not for the presence of an adjacent (back-door) cysteine in proximity to the active-site cysteine in the Cdc25's, the sulfenic acid would rapidly oxidize further to the irreversibly inactivated sulfinic acid, as determined by using kinetic partitioning and mass spectrometry with mutants of these back-door cysteines. Thus, the active-site cysteine is protected by rapid intramolecular disulfide formation with the back-door cysteines in the wild-type enzymes. These intramolecular disulfides can then be rapidly and effectively rereduced by thioredoxin/thioredoxin reductase but not glutathione. Thus, the chemistry and kinetics of the active-site cysteines of the Cdc25's support a physiological role for reversible redox-mediated regulation of the Cdc25's, important regulators of the eukaryotic cell cycle.

In recent years, oxidation by reactive oxygen species (ROS)[1] has been added to the growing list of reversible protein modifications involved in signal transduction and cellular regulation that includes phosphorylation, methylation, ubiquitination, nitrosylation, and sumoylation. Originally, ROS were thought to be only harmful byproducts of aerobic processes and/or involved in the phagocytic process of cells such as microbicidal neutrophils. The discovery that there exists a tightly regulated production of ROS at lower levels than those needed for microbicidal function has supported the concept of oxidation as a means of regulation or signal propagation (*1*, *2*). Mild oxidation at low concentrations of ROS leads to the conversion of selected cysteine residues to sulfenic acids (Cys-$SO^-$) or possibly further oxidation products. Not all cysteines, however, are subject to this form of modification because of the low reactivity of the typically protonated thiol (p$K_a$ of ∼8.5) under physiological conditions (pH of 7.2). Susceptible cysteine residues are frequently located within the active sites of proteins, such as the cysteine found in the active-site motif ($HCX_5R$) of the protein tyrosine phosphatases (PTPs) and the dual-specificity phosphatases (DSPs) (*3*). The p$K_a$'s of these cysteine residues are perturbed to the acidic range, as low as 4.7 in the *Yersinia* phosphatase (YOP) (*4*) or 5.8 in the cell cycle phosphatase Cdc25B (*5*), making them much more reactive with ROS. Oxidation of the thiolate form of cysteine, particularly when the modified cysteine is the critical catalytic residue involved in formation of the phosphocysteine intermediate, leads to inactivation of enzymatic activity. Because the formation of sulfenic acids is usually reversible by cellular reductants such as glutathione and thioredoxin, reactivation of the enzyme can occur and thus provide a mechanism for reversible regulation by ROS. Direct evidence supporting the role for reversible oxidation of cysteine residues has been found for the regulation of numerous phosphatases, including PTP1B (*6*−*9*), LMW phosphatase (*10*), PTEN (*11*), and SHP-2 (*12*). On the other hand, because the sulfenic acid is unstable (*13*), further oxidation to the sulfinic acid (Cys-$SO_2^-$) or sulfonic acid (Cys-$SO_3^{2-}$) is also observed, leading to irreversible inactivation of the enzyme. Unexpectedly, recent experiments with

† This work was supported by NIH Grant R01 GM61822-01.

* To whom correspondence should be addressed. Phone: (919) 668-6188. Fax: (919) 613-8642. E-mail: rudolph@biochem.duke.edu.

[1] Abbreviations: ROS, reactive oxygen species; PTPase, protein tyrosine phosphatase; DSP, dual-specific phosphatase; DTT, dithiothreitol; GSH, glutathione; TR, thioredoxin; TRR, thioredoxin reductase; mFP, 3-*O*-methylfluorescein phosphate; 3-C buffer, 3-component buffer; PTP1B, protein tyrosine phosphatase 1B; VHR, vaccinia H1-related phosphatase; KAP, kinase-associated phosphatase; PTEN, phosphatase and tensin homologue; MALDI-MS, matrix-assisted laser desorption ionization mass spectrometry; ESI-MS, electrospray ionization mass spectrometry; WT, wild type.

10.1021/bi0345081 CCC: $25.00 © 2003 American Chemical Society
Published on Web 08/06/2003

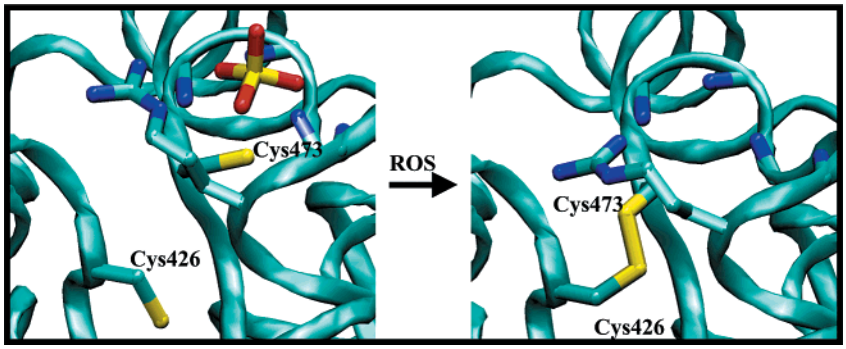


FIGURE 1: Amino acid residues in vicinity of the active site of Cdc25B showing ROS-mediated disulfide bond formation between active-site Cys473 and back-door Cys426. The unoxidized Cdc25B (pdb = 1qb0) is shown with a sulfate anion held in the active-site pocket by the backbone amides of the $HCX_5R$ loop and Arg479. The oxidized form of Cdc25B (pdb = 1cwr) shows the disulfide and the absence of an anion in the active site. The pdb files were taken from ref *38*, and the figure was prepared using VMD (*52*).

peroxiredoxins suggest that sulfenic acids can be rereduced in vivo (*14*).

Recently, a role for oxidation has also been discovered in the regulation of Cdc25C (*15*). Cdc25 phosphatases are critical components of the regulatory machinery of the eukaryotic cell cycle (*16*). There exist three isoforms of Cdc25 phosphatase in humans, Cdc25A, Cdc25B, and Cdc25C. The Cdc25 phosphatases are DSPs and dephosphorylate phospho-Thr14 and phospho-Tyr15 on the Cdk−cyclin complexes. Dephosphorylation of the Cdk−cyclin complexes leads to activation of these regulatory kinases, phosphorylation of their numerous cellular targets, and cell cycle progression. The important role of the Cdc25A and Cdc25B homologues in cell cycle regulation is becoming increasingly apparent as many studies show their increased expression in a wide variety of cancers (*17*−*25*). Additionally, specific phosphatase inhibitors of Cdc25 have been shown to block cell cycle progression (*26*−*29*). Intriguingly, there has been no correlation of Cdc25C overexpression with cancer, even though Cdc25C is generally accepted to be the mitotic Cdc25, the one responsible for progression from G2 to the M phase (*30*).

Previous work has characterized the regulation of Cdc25C during normal cell cycle progression and in response to cellular stress. In these studies, the primary mechanism of control has been found to be via intracellular localization as controlled by phosphorylation of Ser216 and subsequent association with 14-3-3 proteins (*31*−*33*). Additionally, the activity of Cdc25C has been shown to be affected by phosphorylation of Thr48 and Thr67 (*Xenopus* numbering) and subsequent isomerization of the adjacent peptidyl proline bond by Pin1 (*34*). For the Cdc25A homologue, degradation has been shown to be an important mechanism of regulation and subsequent cell cycle arrest in response to UV light, ionizing radiation, or stalled replication (*35*−*37*). Now it has been shown that Cdc25C, but not Cdc25A, undergoes oxidation and degradation in response to treatment of cells by hydrogen peroxide (*15*). These studies of endogenous and transfected Cdc25's in HeLa cells demonstrate the requirement for the active-site cysteine (Cys377) as well as a nearby cysteine (Cys330) in the oxidation-mediated instability of Cdc25C.

As members of the DSP family of phosphatases, the Cdc25's contain the characteristic active-site motif ($HCX_5R$) although their catalytic domains show no structural homology to other members of the PTP or DSP family. An interesting feature of the Cdc25's is the presence of an additional cysteine residue (back-door cysteine) within a DCR motif that is conserved in all known Cdc25's. In Cdc25B, back-door Cys426 is completely buried and is located 4.6 Å from the active-site cysteine (*38*). These back-door cysteines (Cys384 in Cdc25A and Cys330 in Cdc25C) have been shown to form intramolecular disulfides in alternate structures of both Cdc25A and Cdc25B (Figure 1) (*38*, *39*). In the case of Cdc25A, this intramolecular disulfide was formed as a result of tungstate treatment, presumably via oxidation to the sulfenic acid and subsequent attack by Cys384. In the case of Cdc25B, the disulfide was observed in a crystal form lacking a bound anion in the active site. Interestingly, these "structural artifacts" are now coupled with evidence suggesting a role for reversible oxidation and intramolecular disulfide formation for Cdc25C (*15*).

However, many questions remain. What is the relative reactivity of the active-site Cys of the Cdc25 compared to other potentially reactive cysteines inside the cell? What is the partitioning ratio between disulfide formation with the back-door Cys compared to oxidation of the sulfenic intermediate to the potentially irreversibly oxidized sulfinic and/or sulfonic forms? Given the conservation of the back-door cysteine, does intramolecular disulfide formation occur at a reasonable rate in Cdc25 so as to allow redox regulation to be reversible? And what are the possible cellular reductants that can restore the catalytic activity of Cdc25 under physiological conditions? In this contribution we investigate the kinetics of oxidation by hydrogen peroxide, of reactivation by reducing agents (DTT, glutathione, and thioredoxin), as well as the role of the additional cysteine in protection against excessive oxidation for Cdc25B and Cdc25C. The chemistry and kinetics of these processes are shown herein to support the idea of a physiological role for reversible redox-mediated regulation of Cdc25 in cell cycle control.

## MATERIALS AND METHODS

*Materials*. Hydrogen peroxide ($H_2O_2$) was obtained from EM Science, and stock solutions of 100 mM were prepared daily. Thioredoxin/thioredoxin reductase (TR/RR) from *Escherichia coli* was a generous gift from JoAnne Stubbe (M. I. T.). NADPH, mFP, DTT, glutathione, mannitol, and catalase were obtained from Sigma. Sequencing-grade trypsin was purchased from Promega.

*Preparation of Cdc25B and Cdc25C*. The catalytic domains of the Cdc25's were prepared as previously described

Scheme 1: Reaction Pathway for Oxidation/Reduction of Active-Site Cys473 and Back-Door Cys426 of Cdc25B[a]

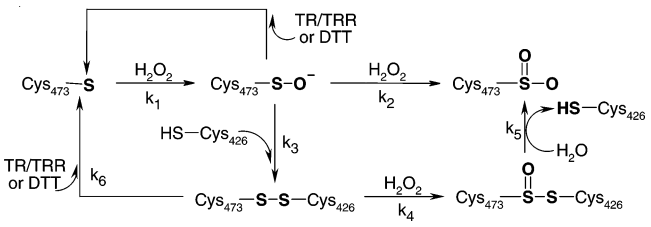


[a] The same pathway, albeit with no evidence supporting steps $k_4$ and $k_5$, can be drawn for Cdc25C where Cys377 is at the active site and C330 is the back-door cysteine.

(*40*, *41*). Mutations of the back-door cysteines for Cdc25B (C426S) and Cdc25C (C330S) were generated using QuickChange mutagenesis (Stratagene) and the following primers: Cdc25B(C426S): GTGATTGTAGACTCCAGATACCCC and GGGGTATCTGGAGTCTACAATCAC; Cdc25C(C330S): TATGTCATTGATTCTCGCTATCC and GCGAGAATCAATGACATAAAAC. The mutant proteins were purified as for the wild type (WT). Enzymes stored in standard TNED buffer (50 mM Tris-HCl, pH 8.0, 50 mM NaCl, 1 mM EDTA, and 1 mM DTT) were dialyzed into 3-C buffer (50 mM Bis-Tris, 50 mM Tris, and 100 mM Na-acetate, pH 7.0) supplemented with one enzyme equivalent of DTT prior to inactivation with hydrogen peroxide.

*Rate of Inactivation*. The rate of inactivation of Cdc25 by hydrogen peroxide was determined using a fixed time-point quench protocol. Cdc25 (13−53 $\mu$M) was incubated with varying concentrations of $H_2O_2$ (0.2−1 mM) in 3-C buffer at 20 °C. At varying time points (10−100 s), an aliquot was taken and diluted (330-fold) into 3-C buffer containing 12.5 units of catalase (should consume 200 nmol $H_2O_2$/s). Phosphatase activities were measured immediately with 30 $\mu$M mFP by using a continuous assay that monitors product formation at 477 nm ($\epsilon = 27\,200$ $M^{-1}$ $cm^{-1}$). The percent remaining activities were determined by comparison with mock-treated samples. The observed rate constant of inactivation $k_{obs}$ was determined by fitting the data to eq 1.

$$\text{percent\_remaining\_activity} = 100\ e^{-k_{obs}t} + \text{remaining\_activity} \quad (1)$$

Control experiments demonstrated that neither the presence of low concentrations of DTT remaining from the storage buffer nor the absolute enzyme concentration altered the observed rate of inactivation. The pseudo-second-order rate constant $k_1$ (Scheme 1) was obtained by fitting the linear dependence of the rate of inactivation on the concentration of $H_2O_2$ (inset of Figure 2). Inactivation in the presence of inorganic phosphate was performed by addition of varying phosphate concentrations from a 1 M stock (pH 7.0). Given that there is no saturating behavior observed for inactivation by $H_2O_2$, the $K_i$ for protection by phosphate was determined by fitting the data to eq 2

$$k_{obs} = k_1[H_2O_2]/(1 + [P_i]/K_i) \quad (2)$$

where $k_1$ is the pseudo-second-order rate constant of inactivation from Figure 2. The $K_i$ for competitive inhibition by phosphate vs the substrate mFP was determined by fitting the data from standard inhibition kinetics (mFP varied from

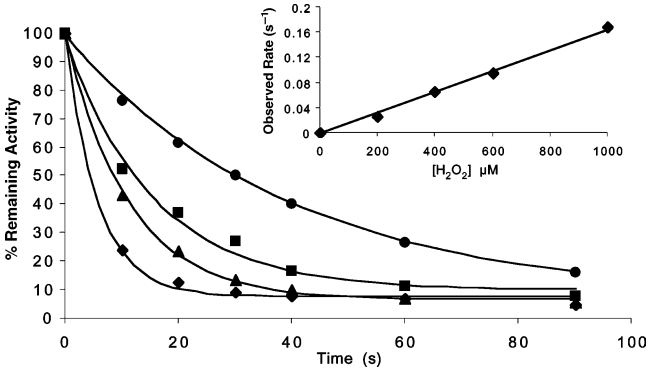


FIGURE 2: Time dependence of Cdc25B inactivation by $H_2O_2$. The reactions were performed as described in the Materials and Methods section. The concentrations of $H_2O_2$ were 200 $\mu$M (●), 400 $\mu$M (■), 600 $\mu$M (▲), and 1 mM (◆). The curves shown are derived from fitting the data to eq 1. The inset shows the concentration dependence of the inactivation used to derive the pseudo-second-order rate constant $k_1$.

2 to 200 $\mu$M and phosphate varied from 0 to 10 mM) to eq 3 using Kinetasyst.

$$v_{obs} = V_{max}[\text{mFP}]/(K_m(1 + [P_i]/K_i) + [\text{mFP}]) \quad (3)$$

*Reversibility and Numerical Integration*. Reversibility was examined as for the inactivation experiments described above by using a partitioning protocol with the inclusion of a 30 min incubation with or without 50 mM DTT in the catalase-containing quench solution. The relative amounts of reversibly inactived Cdc25 (sulfenic and intramolecular disulfide) vs irreversibly inactivated Cdc25 (higher oxidation states) were determined by comparison of the rates of reaction with 30 $\mu$M mFP following further dilution into 3-C buffer. The observed rate of accumulation of unrecoverable activity ($k_{obs}$) was determined by fitting the data to eq 4.

$$\text{percent\_unrecoverable\_activity} = 100(1 - e^{-k_{obs}t}) + \text{remaining\_activity} \quad (4)$$

Control experiments showed that the observed rate was independent of the incubation time with DTT, confirming that our conditions were sufficient to fully rereduce the reversibly oxidized forms. Numerical integration of eqs 5−8 (Scheme 1) were used to model the overall time course of the reaction.

$$\delta[S - O^-]/\delta t = k_1[H_2O_2][S^-] - k_2[H_2O_2][S - O^-] - k_3[S - O^-] \quad (5)$$

$$\delta[S - O_2^-]/\delta t = k_2[H_2O_2][S - O^-] + k_5[S - S{=}O] \quad (6)$$

$$\delta[S - S]/\delta t = k_3[S - O^-] - k_4[H_2O_2][S - S] \quad (7)$$

$$\delta[S - S{=}O]/\delta t = k_4[H_2O_2][S - S] - k_5[S - S{=}O] \quad (8)$$

The numerical integration was separated into parts in various columns of an Excel spreadsheet wherein the exact differential $\delta t$ was replaced with the interval $\Delta t$. The interval $\Delta t = 1$ s was sufficiently small so as to accurately represent a continuous process.

Table 1[a]

| enzyme | $k_1$ ($M^{-1}$ $s^{-1}$) | $k_2$ ($M^{-1}$ $s^{-1}$) | $k_3$ ($s^{-1}$) | $k_4$ ($M^{-1}$ $s^{-1}$) | $k_5$ ($s^{-1}$) | $k_6$ ($M^{-1}$ $s^{-1}$) |
|---|---|---|---|---|---|---|
| Cdc25B | 164 ± 14 | fixed at 60 | 0.16 ± 0.03 | 2.0 ± 0.5 | >0.5 | 1007 ± 18 |
| Cdc25B(C426S) | 190 ± 26 | 47 ± 3 | − | − | − | − |
| Cdc25C | 120 ± 10 | fixed at 110 | 0.012 ± 0.005 | − | − | n.d. |
| Cdc25C(C330S) | 97 ± 8 | 110 ± 30 | − | − | − | − |

[a] Experimentally derived rate constants for the oxidation chemistry of the active-site cysteines of the Cdc25's in accordance with Scheme 1 at 20 °C. The value indicated for $k_6$ is using TR/TRR as the reductant. Some values are not appropriate for the enzyme and reaction studied (−) as, for example, formation of the disulfide with the back-door cysteine mutants. Additionally, inclusion of the step representing the oxidation of the disulfide of Cdc25(WT) to the thiosulfinate was not needed to fit the data and was therefore omitted.

*Reactivation Experiments*. In the reactivation experiments, 54 $\mu$M Cdc25 was incubated with 1 mM $H_2O_2$ for 20 s to inactivate the enzyme. Aliquots were then diluted 33-fold into buffer containing ~1 unit of catalase and varying amounts of different reductants. The reductants included thioredoxin/thioredoxin reductase (TR/TRR, 0.2−5 equiv), dithiothreitol (DTT, 5−50 mM), and glutathione (GSH, 5−50 mM). Experiments with TR/TRR also included NADPH (16−400 $\mu$M), and the ratio of TR to TRR was 250 to 1. Following incubation under reducing conditions for varying times (1−45 min), aliquots were diluted 330-fold into 3-C buffer, and Cdc25 activity was measured using 30 $\mu$M mFP. Control experiments verified that the catalase treatment was necessary and sufficient for inactivating the $H_2O_2$ and that the observed reactivation was independent of NADPH and TRR concentration.

*Mass Spectrometry*. Samples for electrospray ionization mass spectrometry (ESI-MS) were prepared by incubating Cdc25 (6−10 $\mu$g) with or without 1 mM $H_2O_2$ and quenching into 0.1% TFA. Following desalting using a $C_{18}$-ZipTip (Millipore), the sample was directly injected on the API 150EX from Perkin-Elmer SCIEX. Samples for matrix-assisted laser desorption ionization mass spectrometry (MALDI-MS) were prepared by trypsin digestion of ~100 $\mu$g of Cdc25 following treatment with or without 300 $\mu$M $H_2O_2$ for 2 min. The protein was purified through a G-25 column to separate rapidly the protein from excess $H_2O_2$ and then was dialyzed into 50 mM ammonium bicarbonate buffer at pH 7.8. The protein was digested with 2 $\mu$g of sequencing grade trypsin by incubation overnight at 37 °C. The digestion was stopped by addition of the protease inhibitor tosyl lysyl chloromethyl ketone and was desalted with a $C_{18}$-ZipTip. The peptides were analyzed by MALDI-TOF using the Voyager DE-Pro from Applied Biosystems.

## RESULTS AND DISCUSSION

We have used in vitro kinetic experiments to investigate the potential role of reversible ROS-mediated regulation of the active-site cysteine of Cdc25, a dual-specific phosphatase of the PTP family. Although there is a growing body of evidence suggesting the importance of ROS-mediated regulation of PTPs, there has been little consideration of the important kinetic parameters involved in such a process and no direct evidence for the oxidation states of the active-site cysteine in the Cdc25. The kinetic parameters of interest include the absolute and relative rates of the various oxidation steps as well as the rate and mechanism of reversibility, including the identity of the cellular reductant. Below we present data for each of these open questions, detailing the experimental design and results for Cdc25B and also providing data for Cdc25C. We also discuss our results in light of their potential physiological relevance and in comparison to the oxidation/reduction of other cysteine phosphatases.

*Cdc25 Is Rapidly Inactivated by $H_2O_2$.* The rate of inactivation by $H_2O_2$ is the first consideration in thinking about the regulation of Cdc25's by reversible oxidation of the active-site cysteine. Although this cysteine is expected to be ionized in the thiolate form ($pK_a = 5.8$ (*5*)) and thus to be more reactive than the average exposed thiol ($pK_a$ = ~8.5 (*42*)), the intracellular concentration of thiols such as glutathione lies in the millimolar range (*43*) whereas Cdc25 is presumably submicromolar. Thus, the cysteine thiolate of Cdc25 would need to be many times more reactive than other thiols to experience any oxidation at low concentrations of $H_2O_2$. By incubating Cdc25B with varying concentrations of $H_2O_2$ for varying times, followed by dilution into buffer containing catalase to deplete the $H_2O_2$, we found the rate of inactivation of Cdc25B at pH 7.0 and 20 °C to be linearly dependent on $H_2O_2$ concentration with a pseudo-second-order rate constant of 164 ± 14 $M^{-1}$ $s^{-1}$ (Figure 1, Table 1). We believe $H_2O_2$ is the reactive species, as control experiments in the presence of the oxygen scavenger mannitol (25−50 mM) or the divalent metal scavenger EDTA showed no change in the observed rate of inactivation (data not shown). With an expected normal temperature dependence (doubling of rate with every 10 °C), the intrinsic rate of Cdc25B oxidation by $H_2O_2$ is >15-fold faster than the rate of inactivation of PTP1B (18 $M^{-1}$ $s^{-1}$ at 30 °C, pH 7; (*8*)). We speculate that the open and exposed architecture of the active-site region of the Cdc25's compared to the deeper phosphotyrosine binding pocket in PTP1B contributes to this significant difference in the rate of inactivation. Cdc25A (69 ± 9 $M^{-1}$ $s^{-1}$) and Cdc25C (120 ± 10 $M^{-1}$ $s^{-1}$), with highly homologous catalytic domains to Cdc25B (~60% identity), are only slightly less reactive than Cdc25B (Table 1). Given the proximity of the back-door cysteine in the Cdc25's and their involvement in the mechanism of inactivation/reactivation (see below), we also measured the rates of inactivation after mutations of these cysteines in Cdc25B and Cdc25C. Conversion of these cysteines to serine did not change the observed rate of inactivation significantly (Table 1).

Notably, the observed rate of inactivation of 332 ± 35 $M^{-1}$ $s^{-1}$ for Cdc25B measured at 37 °C, pH 6.5, is ~400-fold faster than the rate of oxidation of glutathione (0.87 $M^{-1}$ $s^{-1}$ at 37 °C, pH 7.4 (*44*)). We have confirmed this result by measuring the rate of inactivation of Cdc25 by 1 mM $H_2O_2$ in the presence of an 8000-fold excess of the cellular reductant glutathione (10 mM glutathione vs 13.3 $\mu$M Cdc25B). The observed initial rate constant of inactiva-

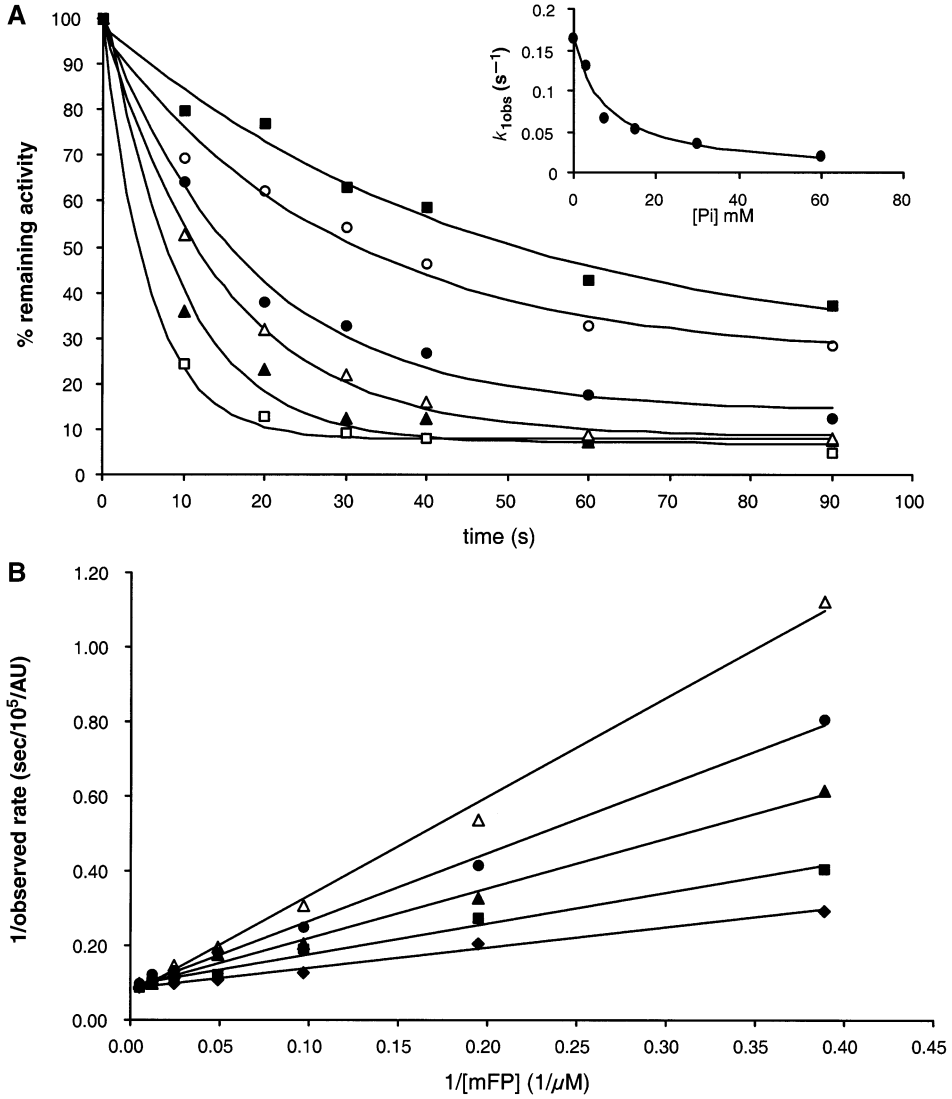


FIGURE 3: (A) Protection of inactivation by phosphate. Variable concentrations of phosphate (0 mM, □; 3.25 mM, ▲; 7.5 mM, △; 15 mM, ●; 30 mM, ○; and 60 mM, ■) were added to an inactivation experiment using 1 mM $H_2O_2$, and the percent remaining activity was measured. The inset shows the data fitted to eq 2, yielding a $K_i$ of 7.6 ± 2.5 mM. (B) Competitive inhibition of phosphate vs mFP for Cdc25B. Reaction rates using varying concentrations of mFP and phosphate (0 mM (◆), 2 mM (■), 4 mM (▲), 7 mM (●), and 10 mM (△)) are shown in a Lineweaver−Burk plot. The lines shown were obtained by fitting the data to eq 3 and yielded a $K_i$ of 2.5 ± 0.5 mM.

tion remained unchanged, as expected, and no modified Cdc25B could be detected by ESI-MS or MALDI-MS following trypsin hydrolysis (data not shown). However, the overall level of inactivation was decreased only 4-fold after 90 s (data not shown). Thus, although glutathione depletes much of the hydrogen peroxide during the time course of the experiment, Cdc25B is still subject to significant inactivation. These results demonstrate that the active site of Cdc25, which has evolved for efficient nucleophilic attack of phosphorylated amino acids, is also highly primed for reaction with and subsequent inactivation by $H_2O_2$. Overall, the very fast inactivation rates we observe bring the relative modification potential of the active sites of the Cdc25's into the realm of physiological possibility despite the intrinsic concentration difference between the Cdc25's and glutathione.

*Oxidation by $H_2O_2$ Is Targeted to the Active-Site Cysteine.* Preliminary experiments measuring the rate of inactivation by $H_2O_2$ with a continuous assay in the presence of the substrate mFP (as described in *8*) yielded a significantly slower rate of inactivation (data not shown). This protection by the substrate suggested that inactivation was taking place at the active-site cysteine, as expected, but was difficult to quantitate given the continuous depletion of substrate during the time course of inactivation. To investigate the protection of the active site more quantitatively, we measured the rate of inactivation by $H_2O_2$ as a function of varying amounts of inorganic phosphate, a competitive inhibitor of mFP (Figure 3). Fitting the data to eq 2 yielded a $K_i$ for phosphate of 7.6 ± 2.5 mM, in reasonable agreement with the determined $K_i$ vs mFP (2.5 ± 0.5 mM). Protection against inactivation by phosphate or substrate has been previously observed for other phosphatases, such as PTP1B and VHR (*8*).

Before proceeding in our kinetic analysis, we used mass spectrometry to confirm that the observed inactivation was due to modification of the cysteine at the active site rather than oxidative damage at other cysteine or methionine residues. To simplify the analysis, we first performed these experiments with the mutant Cdc25B(C426S). (There exist four other cysteine residues in Cdc25B besides active-site Cys473 and back-door Cys426.) Treatment of Cdc25B-(C426S) with $H_2O_2$ for 5−10 min (expected remaining

Table 2: ESI-MS of Cdc25B and Cdc25C[a]

| enzyme | treatment | observed MW | comment |
|---|---|---|---|
| Cdc25B(WT) | none | 22 534 ± 3 | expected MW = 22 538.91 |
| Cdc25B(WT) | $H_2O_2$, 0.5−15 min | 22 539 ± 2 | native, disulfide |
| | | 22 570 ± 3 | sulfinic acid (+32) |
| Cdc25B(C473S) | none | 22 526 ± 3 | expected MW = 22 522.91 |
| Cdc25B(C473S) | $H_2O_2$, 0.5−15 min | 22 525 ± 3 | native |
| Cdc25B(C426S) | none | 22 523 ± 3 | expected MW = 22 522.91 |
| Cdc25B(C426S) | $H_2O_2$, 5−10 min | 22 523 ± 1 | native |
| | | 22 551 ± 3 | sulfinic acid (+32) |
| Cdc25B(C426S) | $H_2O_2$, 15 min | 22 557 ± 3 | sulfinic acid (+32) |
| Cdc25B(C426S) | $H_2O_2$, 0.4−0.5 min | 22 523 ± 2 | native |
| | | 22 540 ± 2 | sulfenic acid (+16) |
| | | 22 561 ± 4 | sulfinic acid (+32) |
| Cdc25C(WT) | none | 22 710 ± 1 | expected MW = 22 709.21 |
| Cdc25C(WT) | $H_2O_2$, 5−10 min | 22 707 ± 2 | native |
| | | 22 736 ± 3 | sulfinic acid (+32) |
| Cdc25C(C330S) | none | 22 695 ± 3 | expected MW = 22 693.51 |
| Cdc25C(C330S) | $H_2O_2$, 5−10 min | 22 697 ± 2 | native |
| | | 22 723 ± 3 | sulfinic acid (+32) |

[a] All mass determinations reported in Da were performed at least in duplicate.

Table 3: MALDI-MS of Cdc25B[a]

| enzyme | back-door peptide | active-site peptide | cross-linked disulfide |
|---|---|---|---|
| Cdc25B(WT) | FVIVDCR | VILIFHCEFSSER | − |
| untreated | 851.5 ± 1.3 | 1579.7 ± 0.5 | |
| Cdc25B(WT) | FVIVDCR | VILIFHCEFSSER | FVIVDCR |
| $H_2O_2$, 1 min | 852.2 ± 1.4 | 1612.3 ± 1.1 | \| |
| | (unchanged) | (sulfinic) | VILIFHCEFSSER |
| | | | 2430.6 ± 0.9 |
| Cdc25B(C426S) | FVIVDSR | VILIFHCEFSSER | − |
| untreated | 836.4 | 1579.6 | |
| Cdc25B(C426S) | 836.4 | 1613.3 | − |
| $H_2O_2$, 1 min | (unchanged) | (sulfinic) | |

[a] All mass determinations reported in Da were performed in duplicate for Cdc25B(WT) and once for Cdc25B(C426S) and deviate less than 1.5 Da from the expected masses.

activity = 5%) followed by quenching in trifluoroacetic acid and ESI-MS showed both a native mass and a mass increase consistent with addition of two oxygens (Table 2). There was no change in mass seen for comparable treatment of the active-site mutant C473S (Table 2). This suggested either the formation of two sulfenic acids on two different cysteines or the formation of a sulfinic acid on one cysteine. Digestion of the $H_2O_2$-treated Cdc25B(C426S) with trypsin followed by MALDI-MS yielded a dominant tryptic peptide of mass 1612 Da corresponding to the peptide VILIFHCEFSSER with two extra oxygens (Table 3). By comparison, the tryptic peptide containing the back-door cysteine (Table 3) and all the other peptides within the range of detection representing the rest of Cdc25 (>85% coverage, data not shown) remained unmodified. These data provide the first unambiguous evidence that $H_2O_2$ is reacting with active-site Cys473, and rapidly forming the irreversibly inactivated sulfinic acid species without oxidation at other residues. Even extensive incubation with $H_2O_2$ that converted all of Cdc25B(C426S) to the sulfinic acid form did not yield any other higher-molecular weight forms (Table 2). We were able to observe the intermediate sulfenic acid form by ESI-MS (Table 2) only upon using shorter incubation times with $H_2O_2$ that were optimized for the presence of this species as determined by our kinetic analyses (see below). Similar results were found for Cdc25C(C330S) but not for the active-site mutant Cdc25B(C473S) (Table 2). These data are in contrast to what has been found for PTP1B and VHR, where there appears to be stable formation of the sulfenic acid without further oxidation to the sulfinic acid (*8*). These observed differences in reactivity between Cdc25 and the other phosphatases may be related to the observed higher intrinsic reactivity toward

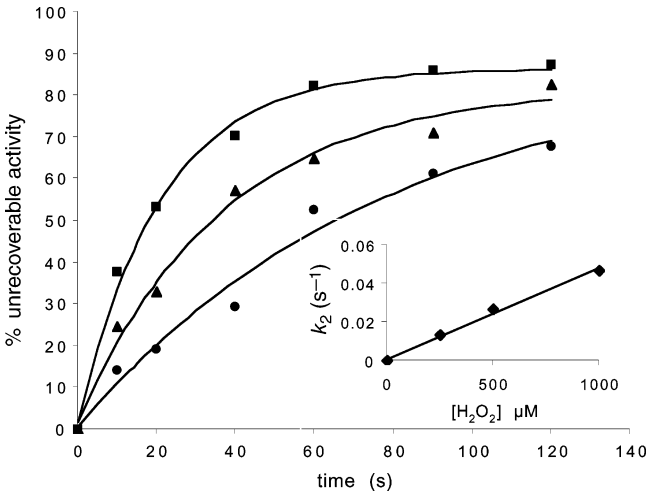


FIGURE 4: Time dependence of irreversible inactivation of Cdc25B-(C426S) by $H_2O_2$. The reactions were performed as described in the Materials and Methods section. The concentrations of $H_2O_2$ were 250 $\mu$M (●), 500 $\mu$M (▲), and 1 mM (■). The curves shown are derived from fitting the data to eq 1. The inset shows the concentration dependence of the inactivation used to derive the pseudo-second-order rate constant $k_2$.

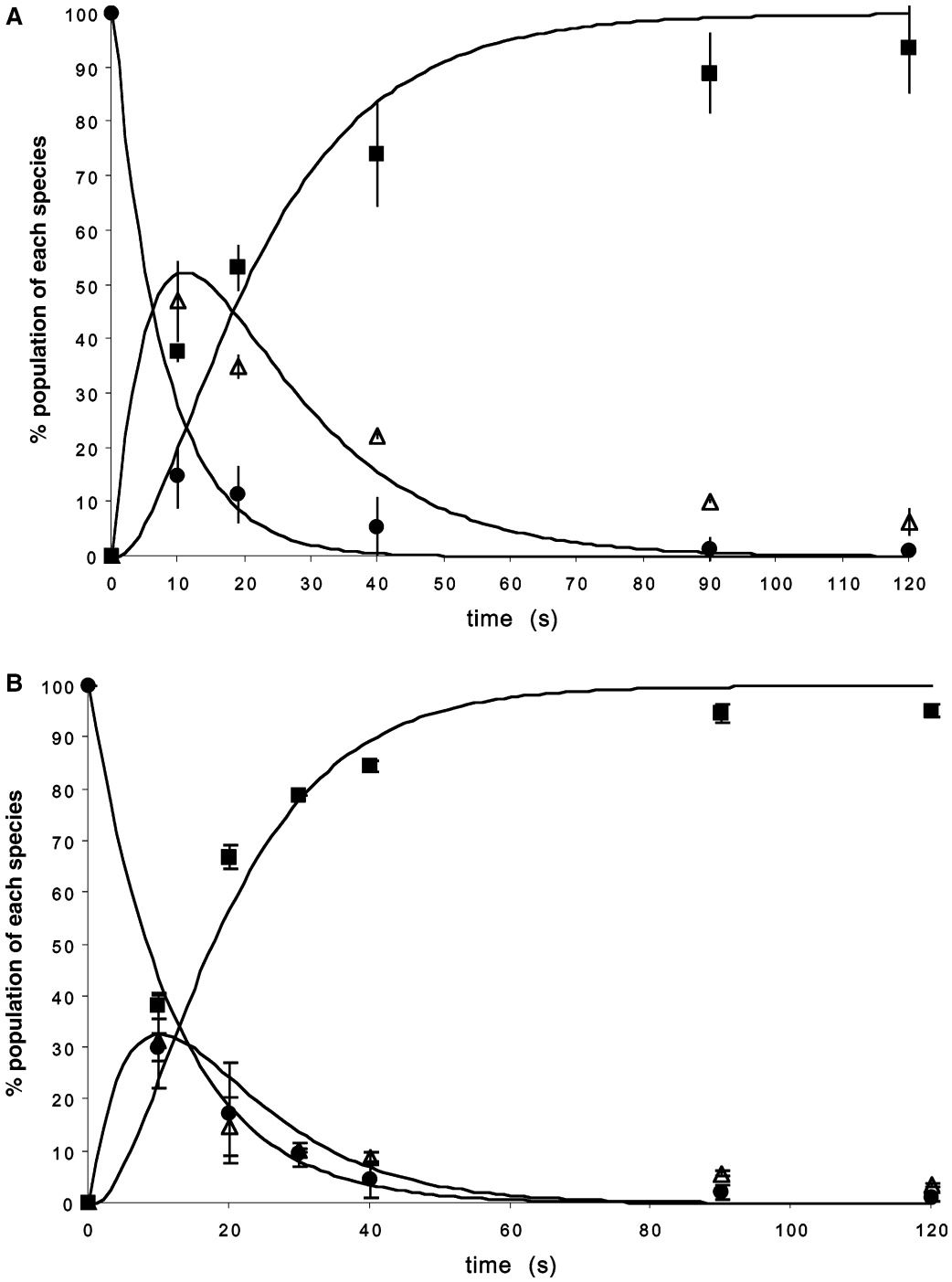


FIGURE 5: Time course for depletion of the free thiolate (●), transient formation of the sulfenic acid (△), and accumulation of the sulfinic acid (■) following treatment of (A) Cdc25B(C426S) or (B) Cdc25C(C330S) with 1 mM $H_2O_2$. The data and simulated curves were generated as described in the Materials and Methods section using $k_1 = 130\ M^{-1}\ s^{-1}$, $k_2 = 60\ M^{-1}\ s^{-1}$ for Cdc25B(C426S) and $k_1 = 80\ M^{-1}\ s^{-1}$, $k_2 = 110\ M^{-1}\ s^{-1}$ for Cdc25C(C330S).

$H_2O_2$ of the cysteine thiolate in the Cdc25's compared to that of the PTP1B and VHR.

Mass spectrometry experiments were also performed with Cdc25B(WT). ESI-MS of Cdc25B(WT), following the same treatment, also showed a mixture of Cdc25, some with an unchanged molecular weight and with an additional two oxygens (Table 2). However, neither the sulfenic acid intermediate nor complete conversion to the sulfinic acid form was observed for Cdc25B(WT). Similar results were observed for Cdc25C(WT) (Table 2). These data are consistent with protective intramolecular disulfide formation between active-site Cys473 and back-door Cys426. MALDI-MS of Cdc25B(WT) confirmed this interpretation (Table 3). Following treatment by $H_2O_2$, the sulfinic acid form of the active-site peptide was detected along with the disulfide-linked peptide derived from the active site and the back-door cysteine.

*Transient Formation of the Sulfenic Acid.* Given our observation of the sulfinic acid as the terminally oxidized form and the transient formation of the sulfenic acid, we next set out to determine the relative rates of oxidation from the sulfenic to the sulfinic acids (Scheme 1). Again, we began

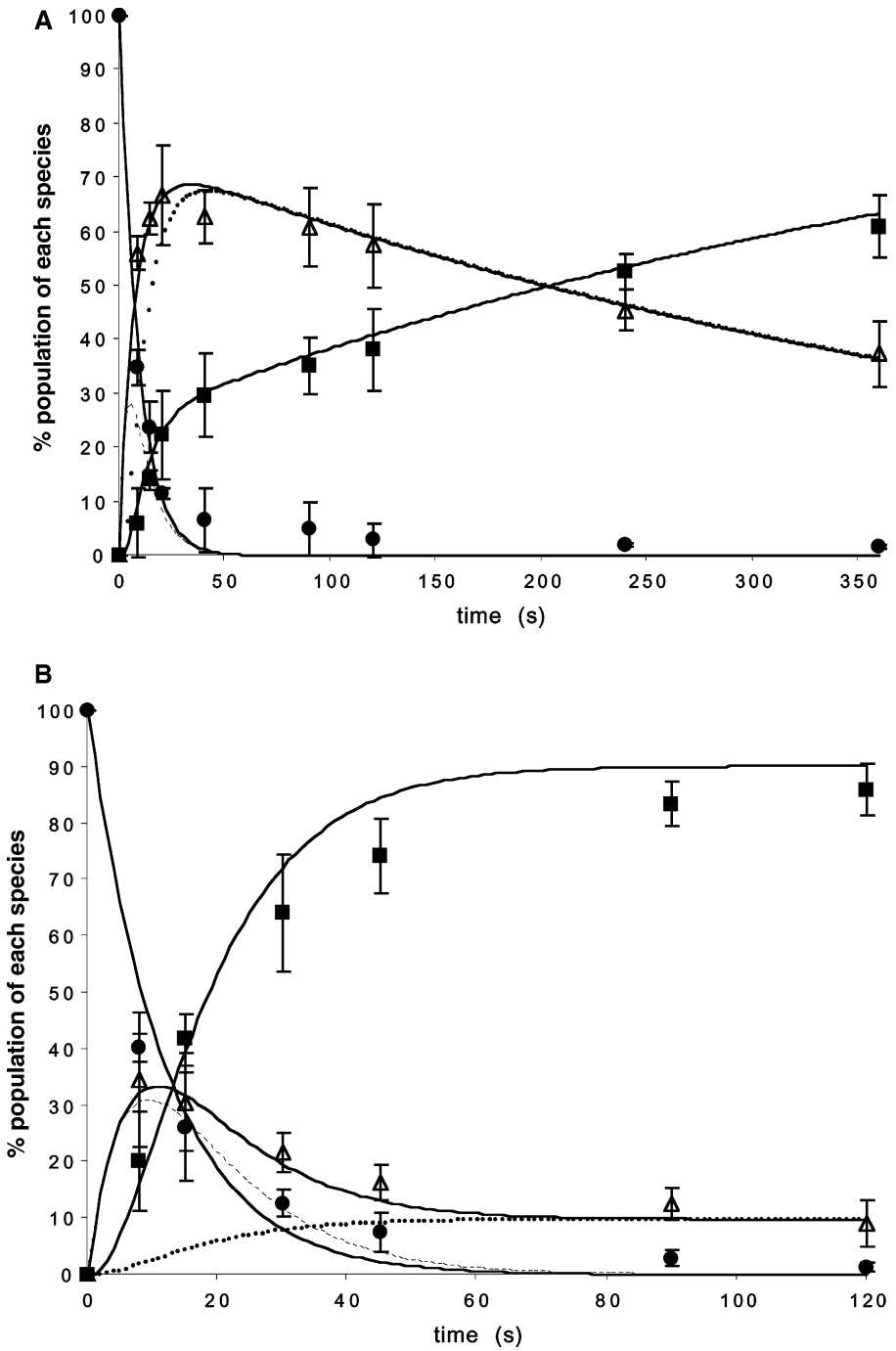


FIGURE 6: Time course for depletion of the free thiolate (●), formation of the sulfenic acid and intramolecular disulfide (△), and accumulation of higher oxidation states (■) following treatment of (A) Cdc25B(WT) and (B) Cdc25C(WT) with 1 mM $H_2O_2$. The data and simulated curves were generated as described in the Materials and Methods section using $k_1 = 130$ $M^{-1}$ $s^{-1}$, $k_2 = 60$ $M^{-1}$ $s^{-1}$, $k_3 = 0.16$ $s^{-1}$, $k_4 = 1.7$ $M^{-1}$ $s^{-1}$, and $k_5 = 0.5$ $s^{-1}$ for Cdc25B(WT) and $k_1 = 80$ $M^{-1}$ $s^{-1}$, $k_2 = 110$ $M^{-1}$ $s^{-1}$, and $k_3 = 0.012$ $s^{-1}$ for Cdc25C(C330S). The dashed line indicates the transient sulfenic acid intermediate, and the dotted line indicates the intramolecular disulfide species.

our analysis using the back-door mutant of Cdc25B as there is, again, no competing disulfide formation to complicate the analysis. To distinguish between these two oxidized forms, we took advantage of the reversibility of the sulfenic form. Aliquots of enzyme incubated with varying concentrations of $H_2O_2$ were diluted into buffer containing excess DTT and catalase or catalase alone. Following a further incubation to allow for DTT-dependent reactivation of the sulfenic form, the ratio of Cdc25 activities was measured using mFP to determine the relative pool of sulfenic and sulfinic species at the time of dilution. The observed rate of appearance of the sulfinic species was then fitted to eq 4 to derive $k_2$, the pseudo-second-order rate constant for conversion of the sulfenic to the sulfinic species where the dependence on $H_2O_2$ was again shown to be first order (Figure 4). The calculated rate constant $k_2$ for Cdc25B(C426S) is $47 \pm 3$ $M^{-1}$ $s^{-1}$, approximately 4-fold slower than $k_1$ (Table 1). Similar experiments were performed for Cdc25C(C330S), and the derived rate constant for conversion of the sulfenic to the sulfinic acid ($k_2$) was found to be $110 \pm 30$ $M^{-1}$ $s^{-1}$, essentially identical to the rate constant for the first oxidation step (Table 1). As noted above, these observations for the

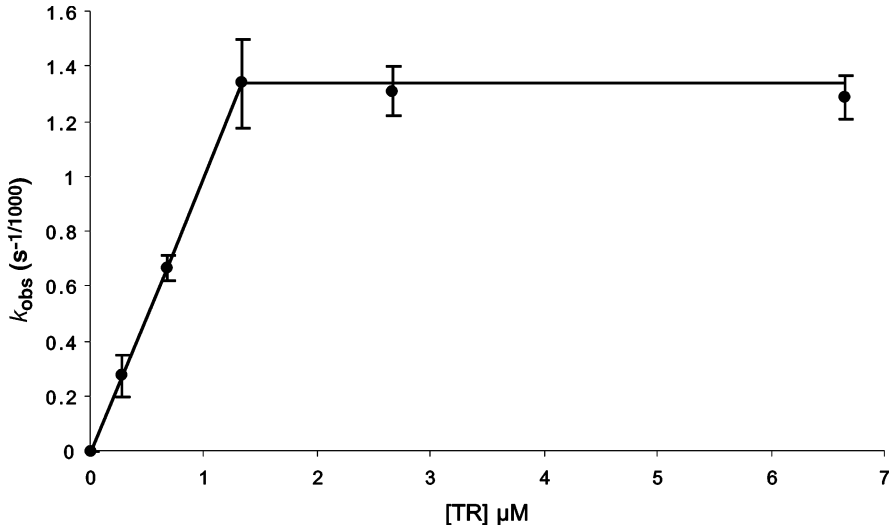


FIGURE 7: Concentration dependence of the rate of reactivation of Cdc25B by TR/TRR at 1.3 $\mu$M Cdc25. The data points below one equivalent of TR to Cdc25 were used to calculate the pseudo-second-order rate constant ($k_6$) of 1007 ± 18 $M^{-1}$ $s^{-1}$.

Cdc25's differ from the apparent stable formation of the sulfenic acid species for PTP1B and VHR as detected by trapping with 7-chloro-4-nitrobenzo-2-oxa-1,3-diazole (*8*).

Using the values for $k_1$ and $k_2$, we plotted and fitted the data for the free thiolate and the sulfenic and sulfinic acids to curves generated by numerical integration of eqs 5−8 (Scheme 1, Figure 5). We note good agreement between the values used to fit the data and the experimentally derived values shown in Table 1 for both the back-door mutants studied, Cdc25B(C426S) and Cdc25C(C330S). Using the knowledge of the relative rates of oxidation, we were able to confirm the existence of the sulfenic acid form as an intermediate by using ESI-MS to minimize the time of oxidation with $H_2O_2$ to 0.4−0.5 min (Table 2). These quantitative experiments demonstrate that the oxidation of the sulfenic to sulfinic acid to yield an irreversibly inactivated form of Cdc25 is a rapid process once the first oxidation has taken place for the mutants of the back-door cysteine. Successful modeling of the reaction time-course with the back-door mutants also set the stage for estimating the rate constants for $k_3$−$k_5$ for the wild-type enzymes.

*Formation of an Intramolecular Disulfide.* We next determined the minimal rate for intramolecular disulfide formation ($k_3$) for Cdc25B(WT) with the assumption that the rate of the conversion of the sulfenic to the sulfinic acid ($k_2$) was unchanged from the Cdc25B(C426S) mutant. By performing the identical partitioning experiment as with the mutant in the preceding paragraph, we were able to derive the relative amounts of irreversibly vs reversibly inactivated enzymes. In this case, the reversibly inactivated enzymes included both the intramolecular disulfide form and the sulfenic acid species. We then modeled the relative reaction rates by using a numerical integration (Figure 6A). Given that we observe a slow accumulation of irreversibly inactivated enzymes with a concomitant decrease in the amount of reversibly inactivated Cdc25, we needed to include oxidation and subsequent hydrolysis of the highly unstable thiosulfinate ($k_4$ and $k_5$) to adequately fit the data for Cdc25B but not for Cdc25C (Scheme 1). The ESI-MS and MALDI-MS results (Tables 2 and 3, respectively) support our interpretation of a significant buildup of the reversibly inactivated disulfide (no MW change in ESI, cross-linked peptide in MALDI) and an irreversibly inactivated sulfinic acid (MW = +32 Da). Thus, the rate of disulfide formation must be at least 3-fold faster than oxidation of the sulfenic to the sulfinic acid under our reaction conditions (1 mM $H_2O_2$) (Table 1). Given that intramolecular disulfide formation is a unimolecular reaction, this protective effect will be even more significant at more physiological concentrations of $H_2O_2$ (e.g., 60-fold at 50 $\mu$M $H_2O_2$). Additionally, we note that oxidation of the disulfide to the thiosulfinic acid is relatively slow, even in the presence of 1 mM $H_2O_2$. Thus, this side reaction is not expected to be physiologically relevant. Cdc25C yielded similar reactivation kinetics, albeit with a significantly reduced trapping ratio for the back-door cysteine and no detectable oxidation of the intramolecular disulfide (Table 1, Figure 6B). In fact, the experimental evidence from treatment of HeLa cells with $H_2O_2$ suggests that this exact process occurs in vivo: ineffective trapping of Cdc25C leads to specific targeting of the enzyme for nonproteosomal degradation (*15*). Overall, these experiments with wild-type Cdc25 clearly demonstrate that disulfide formation in the wild-type enzyme is an effective route for escaping the irreversible end product of the sulfinic acid, in particular for Cdc25B.

Interestingly, the active-site cysteines from two other structurally distinct phosphatases have been shown to form intramolecular disulfides, lending additional support for a physiological role for intramolecular disulfide formation. Treatment of the tumor suppressor PTEN with $H_2O_2$ leads to a reversible disulfide between Cys124 and Cys71 as shown using mass spectrometry (*11*). The crystal structure of KAP phosphatase shows a stable disulfide between active-site Cys140 and back-door Cys79 that appears to account for the low activity of this phosphatase as shown using the back-door mutant (*45*). Although intramolecular disulfide formation has been seen for the Cdc25, PTEN, and KAP phosphatases and the DCR motif is completely conserved in all known Cdc25's (30+ eukaryotes), there appears to be no common sequence motif associated with the back-door cysteine. Additionally, it is clear from the structures of other cysteine phosphatase, e.g., PTP1B, VHR, and MAP kinase phosphatase, that a back-door cysteine is not a universally conserved feature of all cysteine phosphatases.

*Reactivation by Reduction of the Intramolecular Disulfide.* Having established the kinetic competence of protective disulfide formation for Cdc25(WT) in response to treatment with $H_2O_2$, we next investigated the rereduction and reactivation of Cdc25. The intramolecular disulfide bond is considered to be relatively stable, yet susceptible to attack by a thiolate anion for thiol-disulfide exchange. On the other hand, the sulfenic acid that results from active-site oxidation in PTP1B is quite unstable and readily reacts with any vicinal thiols (*13*). Whereas DTT (p$K_a$ 9.2) with its small size and two thiols was a useful tool for elucidating the kinetics of inactivation and reactivation ($k_6 = 0.5 \pm 0.1$ $M^{-1}$ $s^{-1}$) (Scheme 1, Table 1), we turned to cellular reductants with physiological relevance for these studies. GSH and TR/TRR present at 1−10 mM and 1−5 $\mu$M levels, respectively, are the two most important species to consider (*43*, *46*). Very high concentrations of glutathione (up to 50 mM) were very poor at reactivating Cdc25B, yielding only about 30% recovery at a rate significantly slower than DTT (data not shown). Additionally, using ESI-MS, we were unable to detect singly or multiply glutathionylated Cdc25B even after incubation with 50 mM GSH for 30 min (data not shown), in contrast to what has been observed for PTP1B (*9*). Glutathione's poor reactivity with Cdc25 may be the result of its high p$K_a$ of 8.7 and its steric bulk in comparison to DTT.

On the other hand, TR/TRR (derived from *E. coli*) proved to be a rapid and effective reactivator of Cdc25B (Figure 7, Table 1). Concentration-dependent studies with substoichiometric TR yielded a pseudo-second-order rate constant ($k_6$) of $1007 \pm 18$ $M^{-1}$ $s^{-1}$, 2000 times faster than DTT (Table 1). Once one equivalent of TR vs Cdc25B was present, no increase in the apparent rate of reactivation was observed. We did not determine $k_6$ for Cdc25C, given the low concentrations of the intramolecular disulfide form that can be easily obtained in vitro. TR contains two cysteines in close proximity within its active site (CxxC motif). The more reactive thiol of the active-site cysteines of TR has a reduced p$K_a$ of 7.5 and is thus more likely to exist as a thiolate form, the reactive nucleophile required for initiating thiol-disulfide exchange (*47*). On the basis of the even lower p$K_a$ of 6.3 for human TR, we expect the reduction of Cdc25 with its natural reductant to be even faster (*48*). For these reasons, TR/TRR is the most efficient and probable in vivo reductant for Cdc25, as has also been seen for PTEN (*11*).

It should be remembered at this point that Cdc25 is required for cell cycle progression, and that overexpression of Cdc25A and Cdc25B is associated with aggressive tumor growth for a variety of cancers (*17*−*25*). TR is also overexpressed in many different cancers, and it has also been linked to tumor growth (*49*−*51*). One might speculate that TR's growth-promoting effect could be partially exerted by keeping Cdc25 reduced and active. We are attempting to design quantitative experiments to measure the oxidation status of Cdc25 within the cell to address this possibility more directly.

In summary, we have provided evidence supporting the chemical and kinetic competence for regulation of Cdc25 phosphatases by oxidation. First, the rate of oxidation of the active-site cysteine is 400-fold faster than the major cellular reductant glutathione, demonstrating a high sensitivity of Cdc25 to oxidation. Second, the back-door cysteine, which is conserved in all known Cdc25's, makes for an effective trap of the highly reactive sulfenic acid to yield a reversibly inactivated form of Cdc25, thus minimizing the irreversible formation of the sulfinic acid. Third, the intramolecular disulfide that forms as a consequence of oxidation of the active site is readily reducible by the cellular reductant thioredoxin/thioredoxin reductase.

## ACKNOWLEDGMENT

We thank Yan Tong, Michael Fitzgerald, and George Dubay for excellent assistance with the mass spectrometry and JoAnne Stubbe for the generous gift of TR/TRR.

## REFERENCES

1. Adler, V., Yin, Z., Tew, K. D., and Ronai, Z. (1999) *Oncogene 18*, 6104−6111.
2. Finkel, T. (2000) *FEBS Lett. 476*, 52−54.
3. Jackson, M. D., and Denu, J. M. (2001) *Chem. Rev. 101*, 2313−2340.
4. Zhang, Z. Y., and Dixon, J. E. (1993) *Biochemistry 32*, 9340−9345.
5. Chen, W., Wilborn, M., and Rudolph, J. (2000) *Biochemistry 39*, 10781−10789.
6. Bae, Y. S., Kang, S. W., Seo, M. S., Baines, I. C., Tekle, E., Chock, P. B., and Rhee, S. G. (1997) *J. Biol. Chem. 275*, 10527−10531.
7. Lee, S.-R., Kwon, K.-S., Kim, S.-R., and Rhee, S.-G. (1998) *J. Biol. Chem. 273*, 15366−15372.
8. Denu, J. M., and Tanner, K. G. (1998) *Biochemistry 37*, 5633−5642.
9. Barrett, W. C., DeGnore, J. P., König, S., Fales, H. M., Keng, Y.-F., Zhang, Z.-Y., Yim, M. B., and Chock, P. B. (1999) *Biochemistry 38*, 6699−6705.
10. Chiarugi, P., Fiaschi, T., Taddei, M. L., Talini, D., Giannoni, E., Raugei, G., and Ramponi, G. (2001) *J. Biol. Chem. 276*, 33478−33487.
11. Lee, S.-R., Yang, K.-S., Kwon, J., Lee, C., Jeong, W., and Rhee, S. G. (2002) *J. Biol. Chem. 277*, 20336−20342.
12. Meng, T.-C., Fukada, T., and Tonks, N. K. (2002) *Mol. Cells 9*, 387−399.
13. Allison, W. S. (1976) *Acc. Chem. Res. 9*, 293−299.
14. Woo, H. A., Chae, H. Z., Hwang, S. C., Yang, K.-S., Kang, S. W., Kim, K., and Rhee, S. G. (2003) *Science 300*, 653−656.
15. Savitsky, P. A., and Finkel, T. (2002) *J. Biol. Chem. 277*, 20535−20540.
16. Nilsson, I., and Hoffman, I. (2000) *Prog. Cell Cycle Res. 4*, 107−114.
17. Galaktionov, K., Lee, A. K., Eckstein, J., Draetta, G., Meckler, J., Loda, M., and Beach, D. (1995) *Science 269*, 1575−1577.
18. Kudo, Y., Yasui, W., Ue, T., Yamamoto, S., Yokozaki, H., Nikai, H., and Tahara, E. (1997) *Jpn. J. Cancer Res. 88*, 947−952.
19. Dixon, D., Moyana, T., and King, M. J. (1998) *Exp. Cell Res. 240*, 236−243.
20. Wu, W. G., Fan, Y. H., Kemp, B. L., Walsh, G., and Mao, L. (1998) *Cancer Res. 58*, 4082−4085.
21. Ma, Z.-Q., Chua, S. S., DeMayo, F. J., and Tsai, S. Y. (1999) *Oncogene 18*, 4564−4576.
22. Yao, Y., Slosberg, E. D., Wang, L., Hibshoosh, H., Zhang, Y.-J., Xing, W.-Q., Santella, R. M., and Weinstein, I. B. (1999) *Oncogene 18*, 5159−5166.
23. Cangi, M. G., Cukor, B., Soung, P., Signoretti, S., Moreira, G., Jr., Ranashinge, M., Cady, B., Pagano, M., and Loda, M. (2000) *J. Clin. Invest. 106*, 753−761.
24. Hernández, S., Hernández, L., Bea, S., Pinyol, M., Nayach, I., Bellosillo, B., Nadal, A., Ferrer, A., Fernandez, P. L., Montserrat, E., Cardesa, A., Cardes, E., and Campo, E. (2000) *Int. J. Cancer 89*, 148−152.
25. Hernández, S., Bessa, X., Hernández, L., Nadal, A., Mallofré, C., Muntane, J., Castells, A., Fernandez, P. L., Cardesa, A., and Campo, E. (2001) *Lab. Invest. 81*, 465−473.
26. Wu, F. Y.-H., and Sun, T. P. (1999) *Eur. J. Cancer 35*, 1388−1393.
27. Tamura, K., Rice, R. L., Wipf, P., and Lazo, J. S. (1999) *Oncogene 18*, 6989−6996.

28. Takahashi, M., Dodo, K., Sugimoto, Y., Aoyagi, Y., Yamada, Y., Hashimoto, Y., and Shirai, R. (2000) *Bioorg. Med. Chem. Lett. 10*, 2571−2574.
29. Peng, H., Xie, W., Otterness, D. M., Cogswell, J. P., McConnel, R. T., Carter, H. L., Powis, G., Abraham, R. T., and Zalkow, L. H. (2001) *J. Med. Chem. 44*, 834−848.
30. Millar, J. B. A., Blevitt, J., Gerace, L., Sadhu, K., Featherstone, C., and Russell, P. (1991) *Proc. Natl. Acad. Sci. U.S.A. 88*, 10500−10504.
31. Peng, C.-Y., Graves, P. R., Thoma, R. S., Wu, Z., Shaw, A. S., and Piwnica-Worms, H. (1997) *Science 277*, 1501−1505.
32. Chen, L., Liu, T. H., and Walworth, N. C. (1999) *Genes Dev. 13*, 675−685.
33. Graves, P. R., Lovly, C. M., and Piwnica-Worms, H. (2001) *Oncogene 20*, 1839−1851.
34. Zhou, X. Z., Kops, O., Werner, A., Lu, P.-J., Shen, M., Stoller, G., Küllertz, G., Stark, M., Fischer, G., and Lu, K. P. (2000) *Mol. Cells 6*, 873−883.
35. Mailand, N., Falck, J., Lukas, C., Syljuåsen, R. G., Welcker, M., Bartek, J., and Lukas, J. (2000) *Science 288*, 1425−1429.
36. Molinari, M., Mercurio, C., Dominguez, J., Goubin, F., and Draetta, G. F. (2000) *EMBO Rep. 1*, 71−79.
37. Falck, J., Mailand, N., Syljuåsen, R. G., Bartek, J., and Lukas, J. (2001) *Nature 410*, 842−847.
38. Reynolds, R. A., Yem, A. W., Wolfe, C. L., Deibel, M. R. J., Chidester, C. G., and Watenpaugh, K. D. (1999) *J. Mol. Biol. 293*, 559−568.
39. Fauman, E. B., Cogswell, J. P., Lovejoy, B., Rocque, W. J., Holmes, W., Montana, V. G., Piwnica-Worms, H., Rink, M. J., and Saper, M. A. (1998) *Cell 93*, 617−625.
40. Rudolph, J., Epstein, D., Parker, L., and Eckstein, J. (2001) *Anal. Biochem. 289*, 43−51.
41. Wilborn, M., Free, S., Ban, A., and Rudolph, J. (2001) *Biochemistry 40*, 14200−14206.
42. Barton, J. P., Packer, J. E., and Sims, R. J. (1973) *J. Chem. Soc., Perkin Trans. 2 11*, 1547−1549.
43. Smith, C. V., Jones, D. P., Guenthner, T. M., Lash, L. H., and Lauterberg, B. H. (1996) *Toxicol. Appl. Pharmacol. 140*, 1−12.
44. Winterbourn, C. C., and Metodiewa, D. (1999) *Free Radical Biol. Med. 27*, 322−328.
45. Song, H., Hanlon, N., Brown, N. R., Noble, M. E. M., Johnson, L. N., and Barford, D. (2001) *Mol. Cells 7*, 615−626.
46. Holmgren, A., and Luthman, M. (1978) *Biochemistry 17*, 4071−4077.
47. Dillet, V., Dyson, H. J., and Bashford, D. (1998) *Biochemistry 37*, 10298−10306.
48. Forman-Kay, J. D., Clore, G. M., and Gronenbor, A. M. (1992) *Biochemistry 31*, 3442−3452.
49. Grogan, T. M., Fenoglio-Prieser, C., Zeheb, R., Bellamy, W., Frutiger, Y., Vela, E., Stemmerman, G., Macdonald, J., Richter, L., Gallegos, A., and Powis, G. (2000) *Hum. Pathol. 31*, 475−481.
50. Shao, L., Diccianni, M. B., Tanaka, T., Gribi, R., Yu, A. L., Pullen, J. D., Camitta, B. M., and Yu, J. (2001) *Cancer Res. 61*, 7333−7338.
51. Kakolyris, S., Giastromanolaki, A., Koukourakis, M., Powis, G., Souglakos, J., Sivridis, E., Georgoulias, V., Gatter, K. C., and Harris, A. L. (2001) *Clin. Cancer Res. 7*, 3087−3091.
52. Humphrey, W., Dalke, A., and Schulten, K. (1996) *J. Mol. Graphics 14*, 33−38.

BI0345081